Stem Cell Reports, Volume *6*

Supplemental Information

Cellular Adjuvant Properties, Direct Cytotoxicity of Re-differentiated Vα24 Invariant NKT-like Cells from Human Induced Pluripotent Stem Cells

Shuichi Kitayama, Rong Zhang, Tian-Yi Liu, Norihiro Ueda, Shoichi Iriguchi, Yutaka Yasui, Yohei Kawai, Minako Tatsumi, Norihito Hirai, Yasutaka Mizoro, Tatsuaki Iwama, Akira Watanabe, Mahito Nakanishi, Kiyotaka Kuzushima, Yasushi Uemura, and Shin Kaneko

Figure S1

A

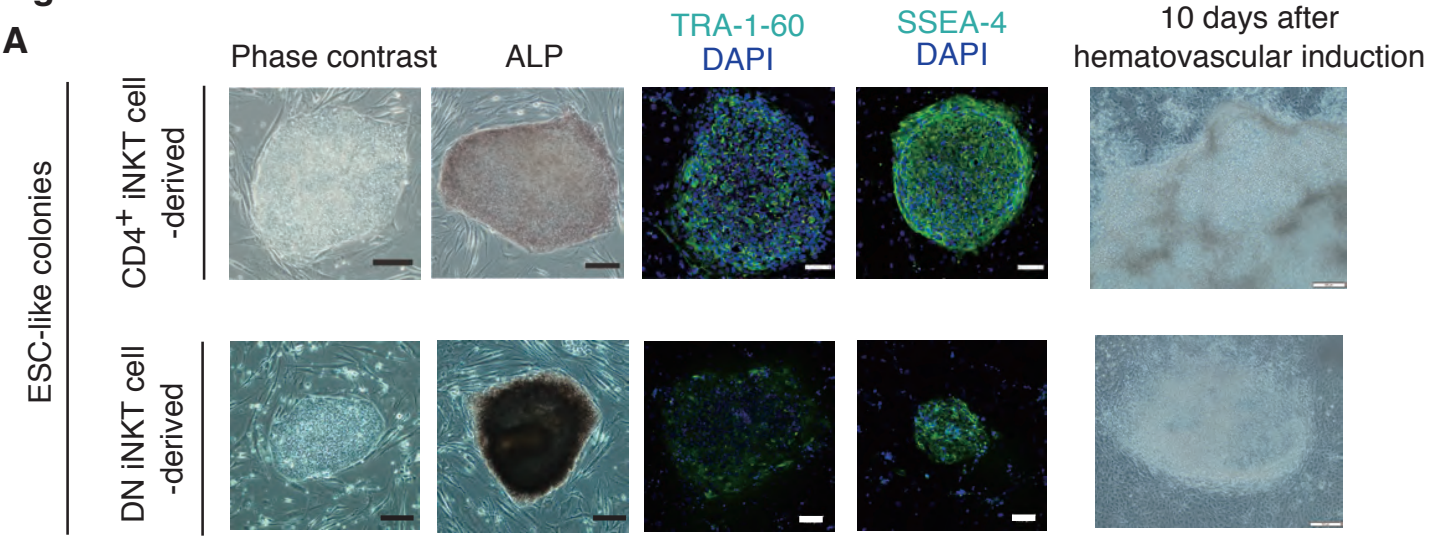

B

Cell source	Donor	Initial cell number ($\times 10^6$)	No. of ESC-like colonies observed at day 21 of induction	No. of transgene-free colonies / No. of colonies picked-up
CD4+ iNKT	A	1.0	82	5 / 5 (100%)
	A	0.5	47	
CD4+ iNKT	B	1.0	>100	6 / 7 (86%)
	B	0.5	>100	
DN iNKT	B	>1.0	38	0 / 6 (0%)
DN iNKT	C	>1.0	63	0 / 24 (0%)

C

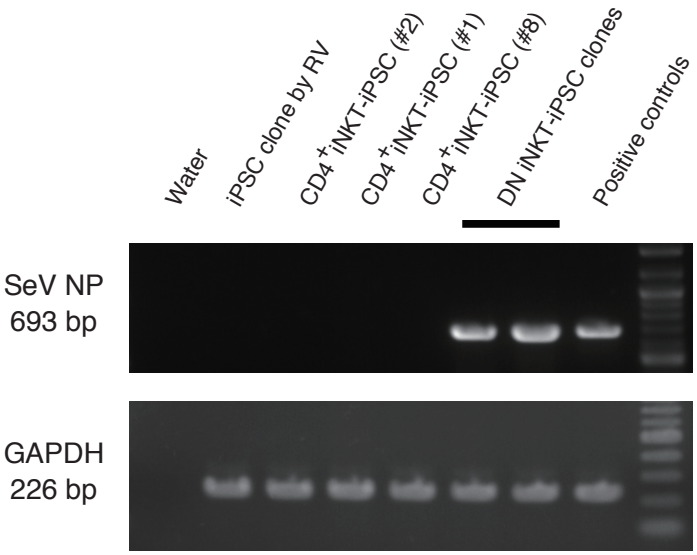

D

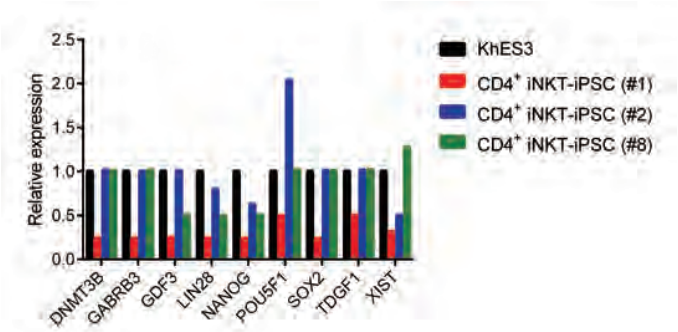

E

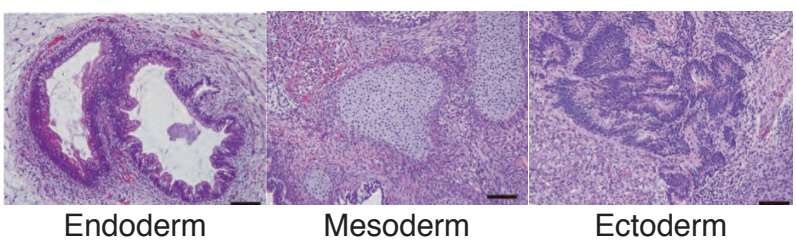

F

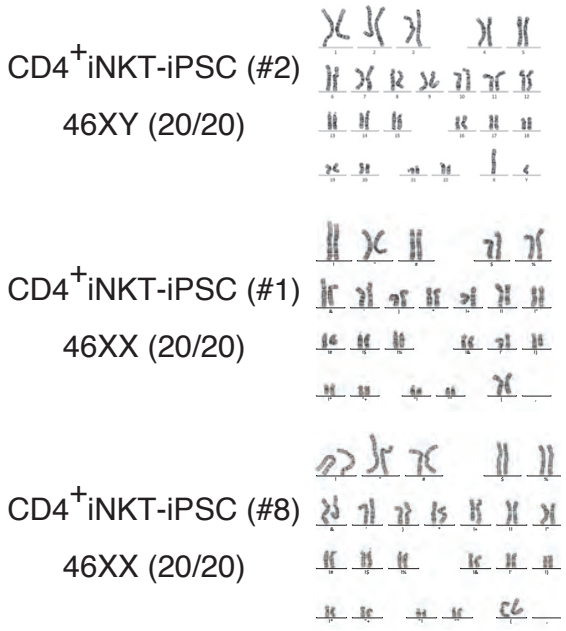

Figure S2

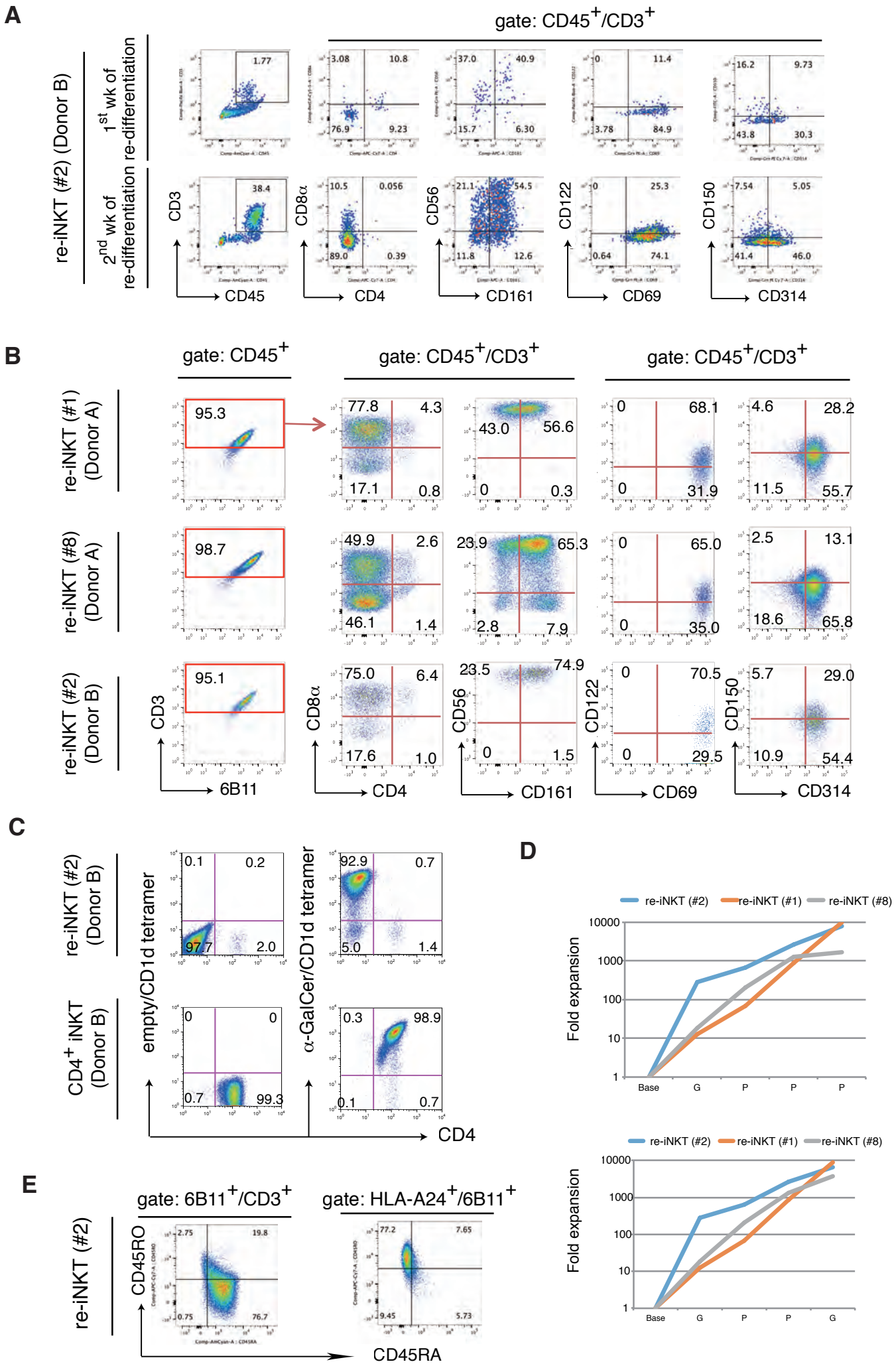
A
gate: CD45+/CD3+
re-iNKT (#2) (Donor B)
1st wk of re-differentiation
2nd wk of re-differentiation
CD3
CD45
CD8α
CD4
CD56
CD161
CD122
CD69
CD150
CD314
B
gate: CD45+
gate: CD45+/CD3+
re-iNKT (#1) (Donor A)
re-iNKT (#8) (Donor A)
re-iNKT (#2) (Donor B)
6B11
C
CD4+ iNKT (Donor B)
empty/CD1d tetramer
α-GalCer/CD1d tetramer
D
re-iNKT (#2)
re-iNKT (#1)
re-iNKT (#8)
Fold expansion
Base
G
P
E
gate: 6B11+/CD3+
gate: HLA-A24+/6B11+
CD45RO
CD45RA

Figure S3

A

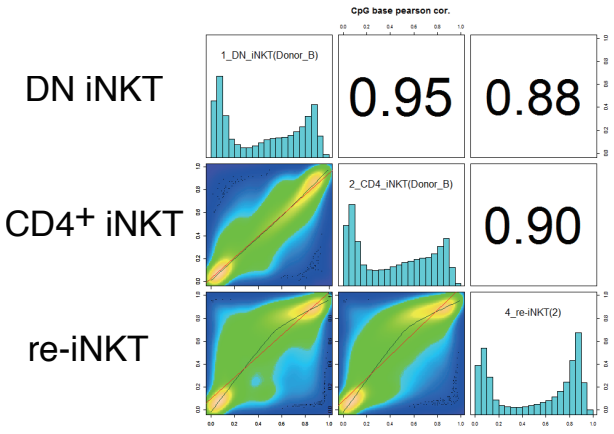
CpG base pearson cor.
DN iNKT
CD4+ iNKT
re-iNKT
1_DN_iNKT(Donor_B)
2_CD4_iNKT(Donor_B)
4_re-iNKT(2)
0.95
0.88
0.90

B

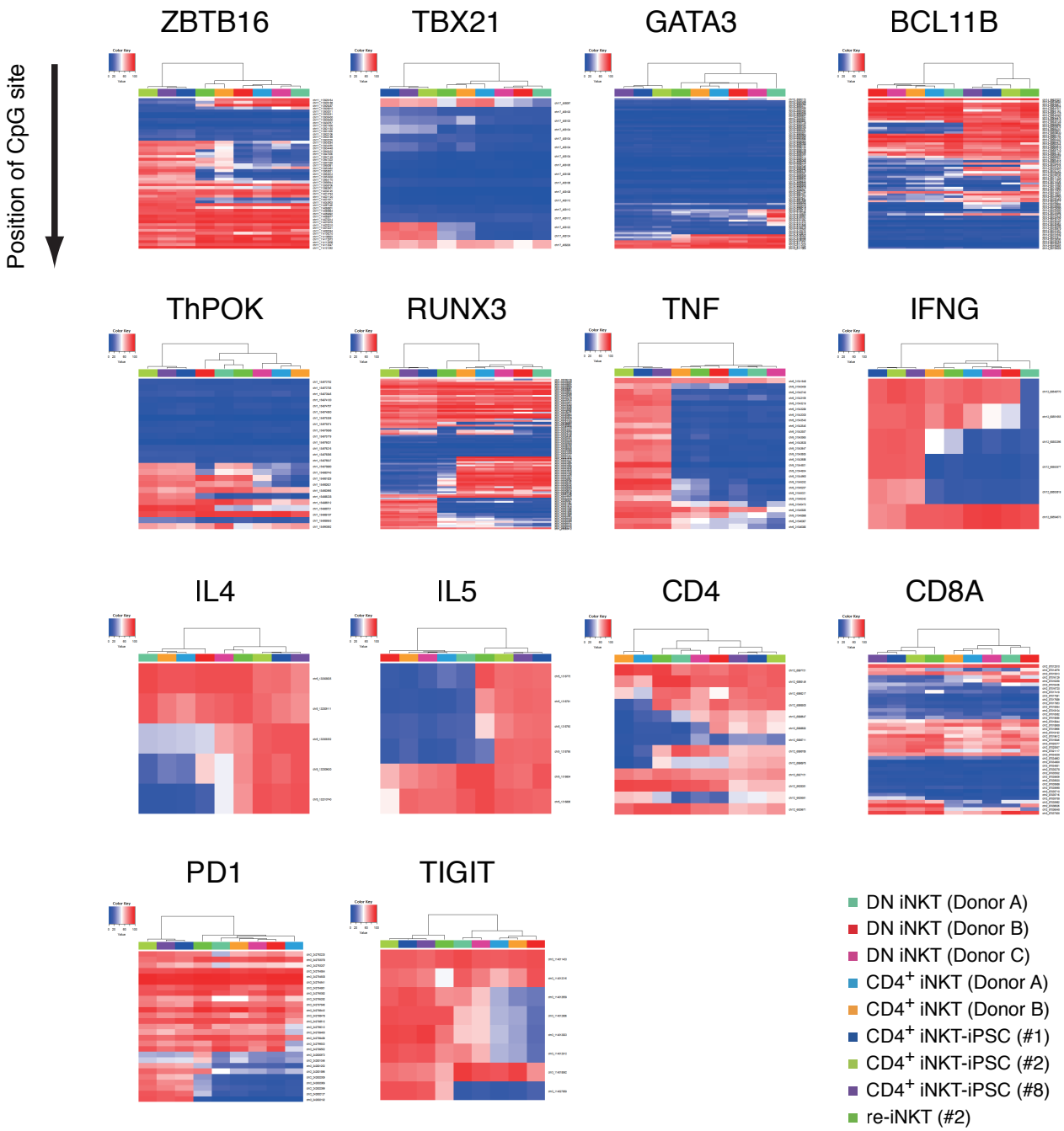
ZBTB16
TBX21
GATA3
BCL11B
Position of CpG site
ThPOK
RUNX3
TNF
IFNG
IL4
IL5
CD4
CD8A
PD1
TIGIT
DN iNKT (Donor A)
DN iNKT (Donor B)
DN iNKT (Donor C)
CD4+ iNKT (Donor A)
CD4+ iNKT (Donor B)
CD4+ iNKT-iPSC (#1)
CD4+ iNKT-iPSC (#2)
CD4+ iNKT-iPSC (#8)
re-iNKT (#2)

Figure S4

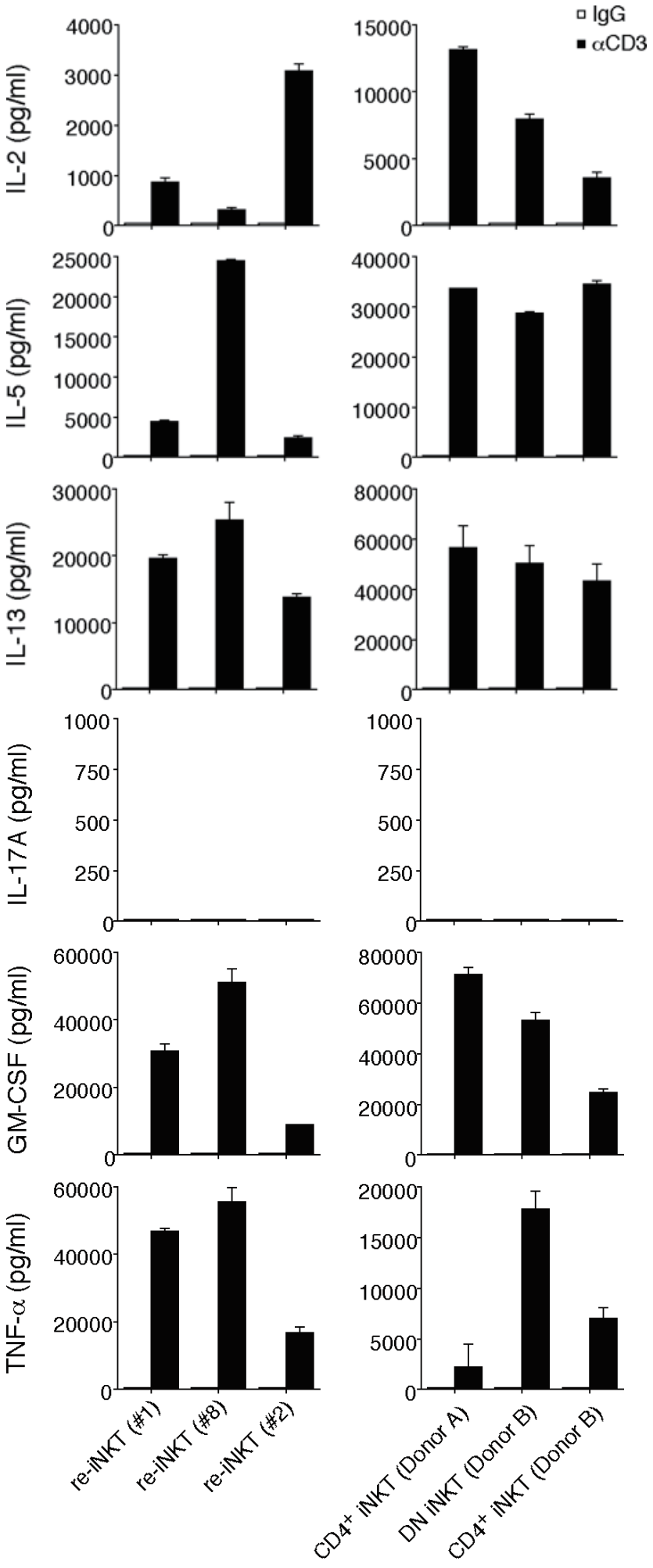
IgG
αCD3
IL-2 (pg/ml)
IL-5 (pg/ml)
IL-13 (pg/ml)
IL-17A (pg/ml)
GM-CSF (pg/ml)
TNF-α (pg/ml)
re-iNKT (#1)
re-iNKT (#8)
re-iNKT (#2)
CD4+ iNKT (Donor A)
DN iNKT (Donor B)
CD4+ iNKT (Donor B)

Figure S5

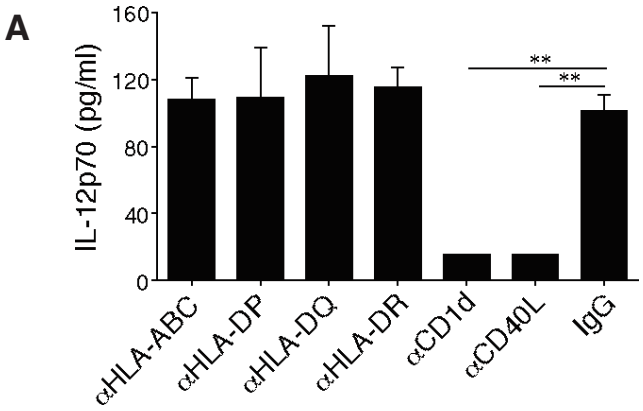
A
IL-12p70 (pg/ml)
160
120
80
40
0
**
**
αHLA-ABC
αHLA-DP
αHLA-DQ
αHLA-DR
αCD1d
αCD40L
IgG

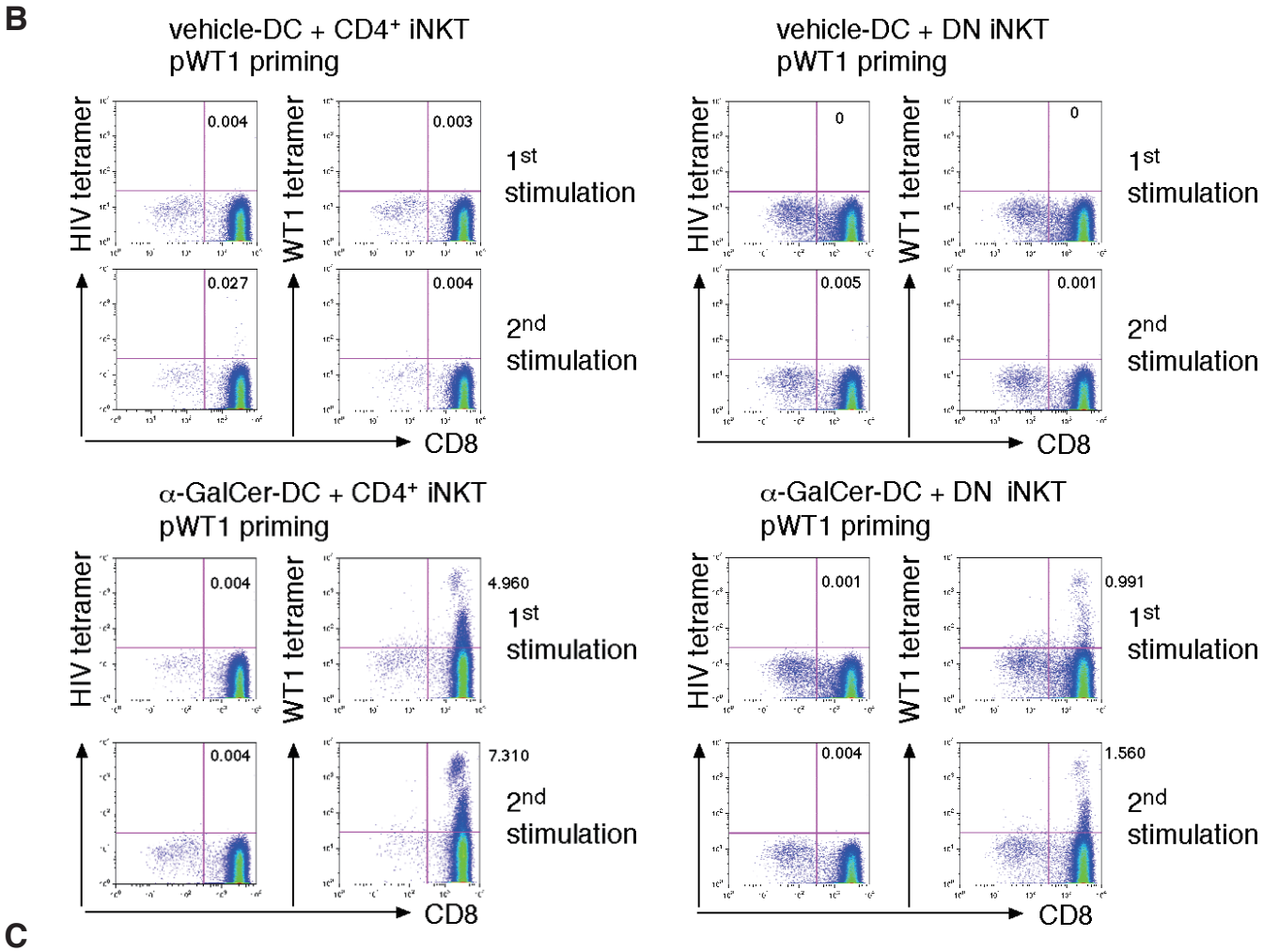
B
vehicle-DC + CD4+ iNKT
pWT1 priming
vehicle-DC + DN iNKT
pWT1 priming
HIV tetramer
WT1 tetramer
0.004
0.003
0.027
0.004
0
0
0.005
0.001
1st stimulation
2nd stimulation
CD8
α-GalCer-DC + CD4+ iNKT
pWT1 priming
α-GalCer-DC + DN iNKT
pWT1 priming
0.004
4.960
0.004
7.310
0.001
0.991
0.004
1.560

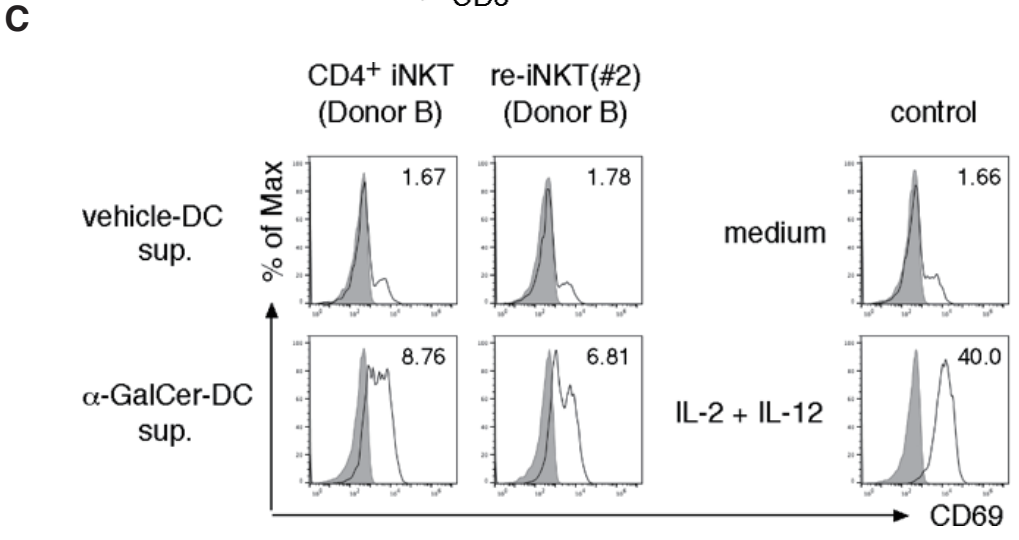
C
CD4+ iNKT
(Donor B)
re-iNKT(#2)
(Donor B)
control
vehicle-DC
sup.
α-GalCer-DC
sup.
% of Max
1.67
1.78
1.66
8.76
6.81
40.0
medium
IL-2 + IL-12
CD69

Figure S6

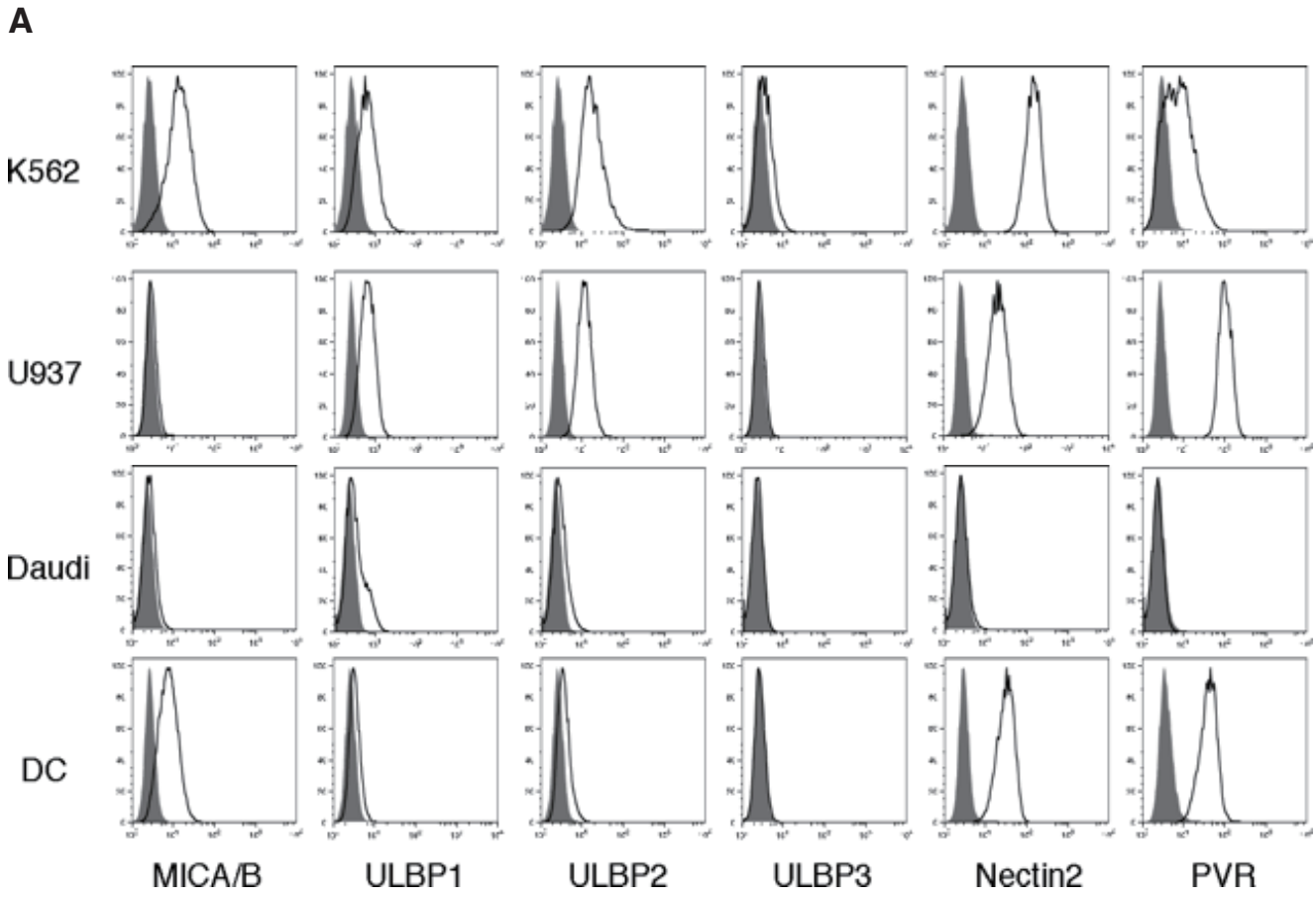
A
K562
U937
Daudi
DC
MICA/B
ULBP1
ULBP2
ULBP3
Nectin2
PVR

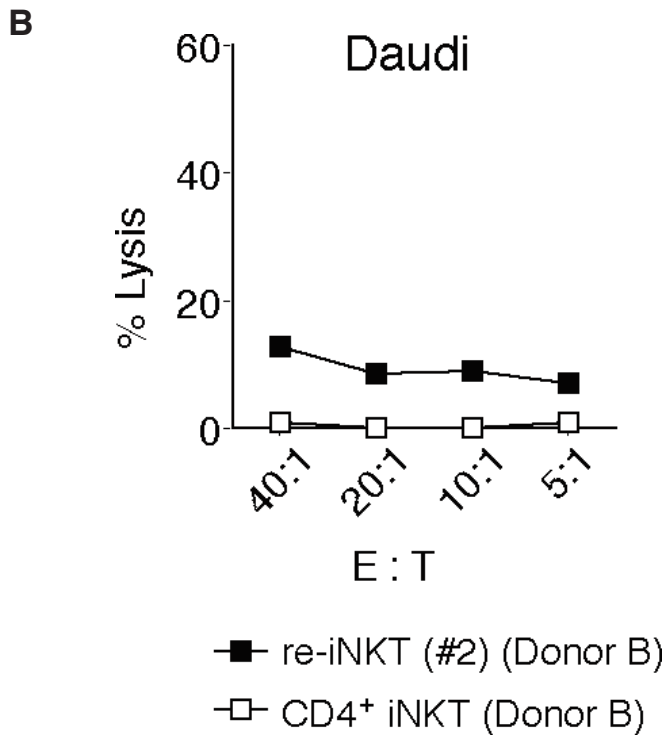
B
Daudi
% Lysis
60
40
20
0
40:1
20:1
10:1
5:1
E : T
re-iNKT (#2) (Donor B)
CD4+ iNKT (Donor B)

Supplemental Information

Supplemental Figure Legends

Figure S1

Generation of iPSCs from human CD4$^+$ iNKT cells

(A) CD4$^+$ and DN iNKT cell-derived ESC-like colonies and sac-like hematopoietic structures derived from the colonies. Shown are phase contrast, alkaline phosphatase stained and immunofluorescent images of representative iNKT cell-derived ESC-like colonies. The upper right image shows hematopoietic cells in a sac-like structure observed in a differentiation culture of CD4$^+$ iNKT-iPSCs. In contrast, no hematopoietic cells were observed in a differentiation culture from DN iNKT-iPSCs. Scale bar = 100 μm. (B) Numbers of ESC-like colonies derived from CD4$^+$ or DN iNKT cells from multiple donors. (C) PCR-based analysis for detection of Sendai virus genomic RNA remnants. No established CD4$^+$ iNKT-iPSC colonies retained remnant Sendai virus. SeV NP, sendai virus vector nucreocapside protein; RV, retroviral vector. (D) Quantitative PCR analysis for the indicated pluripotency-related genes in the indicated human embryonic cell lines. Individual PCR reactions were normalized to 18S ribosomal RNA (rRNA). Relative expression values to embryonic stem cell line KhES3 are indicated. Data was run in triplicate in 2 independent experiments. (E) Representative HE-stained sections of a CD4$^+$ iNKT-iPSC (clone #2)-derived teratoma from a NOD/ShiJic-scid mouse. The iPSCs differentiated into cell lineages derived from endoderm, mesoderm and ectoderm. (F) Karyotype analysis of CD4$^+$ iNKT-iPSCs clones #1 , #2 and #8.

Figure S2, Related to Figure 1:

Phenotypic profile and proliferative potential of re-iNKT cells

(A) Flow cytometric analysis of cells from $CD4^+$ iNKT-iPSC clone #2 on 1^{st} and 2^{nd} week of re-differentiation on OP9/DL1. Shown are the surface protein expression patterns on re-differentiating cells from a representative experiment. (B) Flow cytometric analysis of cells re-differentiating from $CD4^+$ iNKT-iPSC clones #1, #2 and #8 35 days after inducing re-differentiation. Shown are the surface protein expression patterns on re-differentiating cells gated by CD45, CD3 and 6B11. The results are representative of more than 5 independent experiments from the 3 clones and control PBMCs. (C) α-GalCer/CD1d tetramer staining. Re-iNKT cells #2 (upper panels) or parental iNKT cells (lower panels) were stained with negative control CD1d tetramer (left panels) or α-GalCer-loaded CD1d tetramer (right panels) followed by anti-CD4 mAb. (D) Stimulation-mediated expansion of re-iNKT cells. Re-iNKT cells were initially stimulated with α-GalCer-pulsed PBMCs then expanded by PHA-P or α-GalCer-pulsed PBMCs. Shown are representative results from re-iNKT cells derived from the 3 clones. G: α-GalCer, P: PHA-P. (E) Expression profile of CD45RA and CD45RO before (left panel) and after (right panel) α-GalCer stimulation on re-iNKT cells (clone #2).

Figure S3, Related to Figure 2:

DNA methylation profiles of re-iNKT cells

(A) Density plots of DNA methylation levels for DN iNKT (Donor B) vs. $CD4^+$ iNKT (Donor B) (top), DN iNKT (Donor B) vs. re-iNKT (middle), and $CD4^+$ iNKT (Donor B) vs. re-iNKT (botom). Numbers in the panels denote pair-wise Pearson's correlation scores. The histograms on the diagonal describe distributions of CpGs with different DNA methylation levels.

(B) Differential regulation of DNA methylation on differentiation- and function-related genes. Heatmaps visualize DNA methylation levels for each CpG nucleotide (blue, non-methylated; red, methylated). Unsupervised hierarchical clustering of cell samples was performed using the Euclidian distance and Ward's method.

Figure S4, Related to Figure 3:

Cytokine profiles of re-iNKT cells

Re-iNKT cells (2×10^5 cells/well) were stimulated for 24 h with plate-bound control IgG or anti-CD3 mAb (10 μg/ml), after which the levels of the indicated cytokines in the culture supernatant were evaluated using beads-based multiplex immunoassays (left panels). Responses of parental iNKT cells served as references (right panels). Data were run in triplicate, and the experiment was repeated 2 times. The results of 1 representative experiment are shown. Bars depict means ± s.d.

Figure S5, Related to Figure 4:

Induction of tumor Ag-specific CTLs and NK cells via parental iNKT cell-DC interaction

(A) IL-12p70 production by α-GalCer-DCs stimulated by re-iNKT cells in the presence of blocking antibodies. Data were run in triplicate, and experiments were repeated 2 times; the results of 1 representative experiment are shown. Bars depict means ± s.d. (B) α-GalCer-DCs were cultured for 12 h with $CD4^+$ or DN iNKT cells, irradiated and cultured with autologous $CD8^+$ T cells in the presence of $WT1_{235\text{-}243}$ peptide. After 10 days of culture, the frequencies of $WT1_{235\text{-}243}$-specific CTLs were determined by staining for WT1 tetramer (1st stimulation). The cells were then restimulated by irradiated autologous PBMCs pre-pulsed with $WT1_{235\text{-}243}$ peptide.

After an additional 9 days of culture, the frequencies of $WT1_{235-243}$-specific CTLs were determined by staining for WT1 tetramer (2nd stimulation). HIV tetramer served as a negative control. One representative result from at least 2 independent experiments is shown. WT1 peptide-loaded $CD4^+$ and DN iNKT/α-GalCer-DCs induced expansion of WT1-tetramer-positive T cells more efficiently than WT1 peptide-loaded $CD4^+$ and DN iNKT/vehicle-DCs. The cellular adjuvant properties of $CD4^+$ iNKT cells for antigen-specific CTL priming were superior to those of DN iNKT cells. (C) Representative flow cytometry profiles of surface CD69 on $CD3^+CD56^+$ NK cells cultured for 48 h in the presence of 25% cell-free supernatant taken from iNKT-DC coculture. Medium control and IL-2 (300 IU/ml) plus IL-12 (20 ng/ml) control served as references. Open histograms represent staining for CD69; gray histograms represent isotype control.

Figure S6, Related to Figure 5:

Expression of NKG2D ligands and DNAM-1 ligands in leukemic cell lines and DCs

(A) Surface expression of MICA/B, ULBP1, ULBP2 and ULBP3 as NKG2D ligands, and Nectin2 and PVR as DNAM-1 ligands on K562, U937, Daudi and DCs. Shown are representative staining histograms for the indicated surface molecules (open histograms) and isotype-matched controls (filled histograms). (B) Cytotoxicity toward Daudi cells at the indicated E/T ratios. Daudi cells that expressed neither NKG2D ligand nor DNAM-1 ligands had little susceptibility to re-iNKT cell-lysis.

Table S1. The list of genes extracted for Figure 2C

Gene	Accession
ZBTB16	NM_006006+NM_001018011
TBX21	NM_013351
GATA3	NM_002051+NM_001002295
CCDC22+FOXP3	NM_014008+NM_001114377+NM_014009
RORC	NM_005060+NM_001001523
ZBTB7B(ThPOK)	NR_045515+NM_001252406+NR_049765+NM_001256455+NR_046206
RUNX3	NM_004350+NM_001031680
RUNX1	NM_001754+NM_001001890+NM_001122607
BCL11B	NM_138576+NM_022898
TCF7	NM_003202+NM_001134851+NM_201634+NM_201632+NM_213648+NR_033449
ID3	NM_002167
ID2	NM_002166
ETS1	NM_005238+NM_001143820+NM_001162422
ETS2	NM_001256295+NM_005239
LEF1+LEF1-AS1	NM_001130713+NM_001130714+NM_016269+NM_001166119+NR_029374+NR_029373
HES1	NM_005524
SOX13	NM_005686
MYB	NM_001161660+NM_001161656+NM_001130172+NM_001130173+NM_005375+NM_001161658+NM_001161659+NM_001161657
GFI1	NM_001127216+NM_005263+NM_001127215
TAL1	NM_003189
IKZF1	NM_001220767+NM_001220769+NM_001220768+NM_001220766+NM_001220765+NM_001220774+NM_001220773+NM_001220772+NM_001220771+NM_001220770+NM_006060+NM_001220776+NM_001220775
IKZF2	NM_016260+NM_001079526
IKZF3	NM_183232+NM_012481+NM_001257411+NM_001257410+NM_001257409+NM_183229+NM_183228+NM_001257412+NM_183231+NM_183230+NM_001257408+NM_001257413+NM_001257414+NR_047560+NR_047561+NR_047559
TCF12	NM_207038+NM_207036+NM_003205+NM_207037+NM_207040
GATA2	NM_001145662+NM_001145661+NM_032638
CEBPA	NM_004364
SATB1	NM_001195470+NM_002971+NM_001131010
EOMES	NM_005442
RBPJ	NM_005349+NM_203283+NM_015874+NM_203284
STAT5B	NM_012448
TNF	NM_000594
IFNG	NM_000619
IL2	NM_000586
IL4	NM_000589+NM_172348
IL5	NM_000879
IL10	NM_000572
IL13	NM_002188
IL17A	NM_002190
CSF1	NM_000757+NM_172212+NM_172210+NM_172211
CSF2	NM_000758
IL12RB1	NM_005535+NM_153701
IL12RB2	NM_001559+NR_047584+NM_001258214+NM_001258215+NM_001258216+NR_047583
IL17RB	NM_018725
IL23R	NM_144701
IL4R	NM_000418+NM_001257407+NM_001257997+NM_001257406
CXCR3	NM_001142797+NM_001504
CXCR6	NM_006564
IFNGR1	NM_000416
IL15RA	NM_001256765+NM_002189+NM_172200+NM_001243539+NR_046362
IL2RA	NM_000417
IL2RB	NM_000878
IL2RG	NM_000206
IL7R	NM_002185

Table S2. List of antibodies used in this study

Antigen	Clone	Isotype
CD1d	51.1	mouse IgG2b
CD122	TU27	mouse IgG1
CD150	A12(7D4)	mouse IgG1
CD161	HP-3G10	mouse IgG1
CD183(CXCR3)	G025H7	mouse IgG1
CD196(CCR6)	G034E3	mouse IgG2b
CD226(DNAM-1)	11A-8	mouse IgG1
CD226(DNAM-1)	DX11	mouse IgG1
CD279(PD-1)	EH12.2H7	mouse IgG1
CD3	HIT3a	mouse IgG2a
CD3	UCHT1	mouse IgG1
CD314(NKG2D)	1D11	mouse IgG1
CD4	RPA-T4	mouse IgG1
CD40L	TRAP-1	mouse IgG1
CD40L	40804	mouse IgG2b
CD45	HI30	mouse IgG1
CD56	B159	mouse IgG1
CD56	HCD56	mouse IgG1
CD69	FN50	mouse IgG1
CD86	IT2.2	mouse IgG2b
CD8α	3B5	mouse IgG2a
CD8α	SK1	mouse IgG1
CD96	NK92.39	mouse IgG1
FasL	NOK-1	mouse IgG1
FasL	Polyclonal	goat IgG
granzyme B	GB11	mouse IgG1
HLA-A24	17A10	mouse IgG2b
HLA-ABC	W6/32	mouse IgG2a
HLA-DP	B7/21	mouse IgG3
HLA-DQ	SPVL3	mouse IgG2a
HLA-DR	L243	mouse IgG2a
MIC A/B	6D4	mouse IgG2a
nectin-2	TX31	mouse IgG1
NKp44	p44-8	mouse IgG1
NKp46	9E-2	mouse IgG1
perfolin	dG9	mouse IgG2b
PVR	SKII.4	mouse IgG1
TCR Vα24Jα18	6B11	mouse IgG1
TCR Vβ11	C21	mouse IgG2a
TIGIT	MBSA43	mouse IgG1
TNFα	Polyclonal	goat IgG
TRAILR1	Polyclonal	goat IgG
TRAILR2	B-K29	mouse IgG1
ULBP1	170818	mouse IgG2a
ULBP2	165903	mouse IgG2a
CD16	3G8	mouse IgG1

Isotype control	Clone
mouse IgG1	MOPC-21
mouse IgG1	P3.6.2.8.1
mouse IgG2a	G155-178
mouse IgG2b	eBMG2b

Supplemental Experimental Procedures

Cell lines, peptides, cytokines and chemicals

C1R transfectants were established as described (Liu et al., 2008). The cell lines of myelogenous leukemia K562, histiocytic lymphoma U937 and Burkitt's lymphoma Daudi were purchased. HLA-A*24:02-restricted and modified 9-mer Wilms' tumor gene $(WT1)_{235\text{-}243}$ peptide (CMTWNQMNL) was synthesized by Toray Research Center (Kamakura, Japan). Recombinant human (rh) interleukin (IL)-2, rhIL-4 and rh-granulocyte macrophage colony-stimulating factor (GM-CSF) (Primmune, Kobe, Japan), rhIL-12p70 (R&D systems, Minneapolis, MN, USA), and rhIL-7, rhIL-15 and rh fms-related tyrosine kinase 3 ligand (Flt-3L) (Peprotec, UK) were purchased. rh basic fibroblast growth factor (bFGF) and phytohemagglutinin-P (PHA-P) were purchased from WAKO chemical (Osaka, Japan). Vascular endothelial growth factor (VEGF) and rh stem cell factor (SCF) were purchased from R&D systems. Penicillin-killed *Streptococcus pyogenes* (OK432) was purchased from Chugai Pharmaceutical (Tokyo, Japan). α-galactosylceramide (α-GalCer; KRN7000) was purchased from Funakoshi (Tokyo).

Preparation of human monocyte-derived DCs and $CD8^+$ T cells

Human monocyte-derived-DCs were induced as described previously (Liu et al., 2008). Briefly, $CD14^+$ monocytes were isolated from PBMCs using positive magnetic cell sorting with CD14 microbeads (Miltenyi Biotec, Auburn, CA) and cultured at 1.0×10^6 cells/ml in the presence of rhGM-CSF and rhIL-4 (50 ng/ml each). On day 6, nonadherent DCs were harvested and served as immature DCs. $CD8^+$ T cells were isolated from PBMCs by negative magnetic cell sorting using a $CD8^+$ T cell isolation kit (Miltenyi Biotec).

Preparation and activation of NK cells

PBMCs were stimulated with immobilized anti-CD16 mAb in X-VIVO 20 medium (Lonza, Walkersville, MD) supplemented with 5% heat-inactivated human plasma, rhIL-2, and OK432 for 24 h at 39 °C. Then the cells were harvested and cultured in the presence of rhIL-2 at 37 °C. After 10 days of culture, NK cells were isolated using a NK cell isolation kit (Miltenyi Biotec, Bergisch Gladbach, Germany) and cultured for another 10 days. To acquire the resting state, NK cells were cultured for 24 h in the absence of IL-2. Resting state NK cells were cultured for 48 h in the presence of 25% cell-free supernatant taken from iNKT-DC coculture. To prepare supernatant, vehicle or α-GalCer-DCs (1.0×10^6) were cultured with iNKT cells (5.0×10^5) for 24 h.

RT-PCR and Quantitative PCR

Total RNA was extracted from iPSCs using an RNeasy Micro kit (Qiagen) and reverse transcribed using High Capacity cDNA Reverse Transcription kits (Applied Biosystems) with random 6-mer primers. RT-PCR was performed using ExTaq HS (Takara). Individual PCR reactions were normalized against GAPDH rRNA. Primer sequences used in RT-PCR were, 5'-AGACCCTAAGAGGACGAAGA-3' (forward) and 5'-ACTCCCATGGCGTAACTCCATAGTG-3' (reverse) for SeV NP, 5'-GAAGGTGAAGGTCGGAGTC-3' (forward) and 5'-GAAGATGGTGATGGGATTTC-3' (reverse) for GAPDH. Quantitative-PCR was performed using a TaqMan Array Human Stem Cell Pluripotency Card (Applied Biosystems). Individual PCR reactions were normalized against 18S rRNA.

Immunohistochemistry

Human ESC/iPSC colonies fixed in 4% paraformaldehyde were blocked with 8% goat serum and stained with primary antibodies (anti-SSEA-4 1:50, sc-21704, Santa Cruz; anti-TRA-1-60 1:100, MAB4360, Millipore), after which they were stained with secondary antibody (goat anti-mouse IgG, 1:500, A11029, Invitrogen). Nuclei were counterstained with 4', 6-diamidino-2-phenylindol (DAPI; S-1200, Vector Laboratories) according to the manufacturer's instructions. Photomicrographs were taken with a LSM710 confocal microscope (Carl Zeiss).

Teratoma formation

iNKT-iPSC colonies were trypsinized and injected (1.0×10^6 cells/mouse) into the medulla of the testis of NOD/ShiJic-*scid* mice. Nine to twelve weeks after injection, tumors that formed in the testis were extracted, fixed in formalin and embedded in paraffin.

Karyotype analysis

The iPS cell karyotype was determined by LSI Medience Corporation (Tokyo, JAPAN) using the standard staining protocol for Giemsa-banding.

Microarray-based DNA methylation analysis

The EZ DNA methylation kit (Zymo Research, Irvine, CA) was used for bisulfite conversion of 500 ng genomic DNA. Bisulfite-converted DNA was then hybridized to HumanMethylation450 BeadChip (Illumina, San Diego, CA) following the Illumina Infinium HD Methylation protocol. Fluorescent signals were read by iScan (Illumina) and normalized by GenomeStudio V2011.1 (Illumina). DNA methylation levels were calculated by GenomeStudio and are represented as β-values ranging from 0 (non-methylated) to 1 (completely methylated). β-values with detection

P-value ≥ 0.05 and probes whose annotations were not given in RefSeq were removed. Bioinformatic analysis was conducted using R 3.1.0 including R package methylKit (Akalin A, et al., Genome Biol., 2012). The gene region from 1,500 bp upstream of the transcription start site (TSS) to the 3' end of the coding region was subjected to analysis to identify differentially DNA methylated genes. Heatmap visualization and hierarchical clustering were conducted using the heatmap.2 function in gplots and hclust function in R, respectively.

Reference

Akalin, A., Kormaksson, M., Li, S., Garrett-Bakerman, F.E., Figueroa, M.E., Melnick, A., and Mason, C.E.（2012）. methylKit: a comprehensive R package for the analysis of genome-wide DNA methylation profiles. Genome biology *13*, R87

Liu, T.Y., Uemura, Y., Suzuki, M., Narita, Y., Hirata, S., Ohyama, H., Ishihara, O., and Matsushita, S. (2008). Distinct subsets of human invariant NKT cells differentially regulate T helper responses via dendritic cells. European journal of immunology *38*, 1012-1023.